NSWCCD-61-TR—1998/27 Elastic and Plastic Analysis of a Single Edge Cracked Tension Specimen with Clamped Ends

Carderock Division
Naval Surface Warfare Center
Bethesda, MD 20084-5000

NSWCCD-61-TR—1998/27 October 1998

Survivability, Structures, and Materials Directorate
Technical Report

Elastic and Plastic Analysis of a Single Edge Cracked Tension Specimen with Clamped Ends

by

Gerard P. Mercier

REPORT DOCUMENTATION PAGE

Form Approved
OMB No. 0704-0188

1. AGENCY USE ONLY (Leave blank)	2. REPORT DATE	3. REPORT TYPE AND DATES COVERED
	October 1998	Final

4. TITLE AND SUBTITLE
Elastic and Plastic Analysis of a Single Edge Cracked Tension Specimen with Clamped Ends

5. FUNDING NUMBERS
PE 602234N
98-1-6140-254

6. AUTHOR(S)

7. PERFORMING ORGANIZATION NAME(S) AND ADDRESS(ES)
Naval Surface Warfare Center
Caderock Division
9500 MacArthur Blvd.
West Bethesda, MD. 20817-5700

8. PERFORMING ORGANIZATION REPORT NUMBER
NSWCCD-61-TR-1998/27

9. SPONSORING/MONITORING AGENCY NAME(S) AND ADDRESS(ES)
Office of Naval Research
Ballston Center Tower One
800 North Quincy Street
Arlington, VA. 22217-5660

10. SPONSORING/MONITORING AGENCY REPORT NUMBER

11. SUPPLEMENTARY NOTES

12a. DISTRIBUTION/AVAILABILITY STATEMENT

12b. DISTRIBUTION CODE
Distribution Code A

13. ABSTRACT (Maximum 200 words)

An analysis of single edge cracked tension specimens with clamped end conditions was conducted. Single edge tension finite element models at nine crack lengths were constructed and benchmarked against previously accepted analyses with pinloaded boundary conditions. The model boundary conditions were then determined by a direct comparison with experimental strain and displacement data from clamped end specimens. Both the elastic (compliance and elastic stress intensity) and the plastic response (J-plastic, η_{pl}) of the clamped end model were determined at ratios of height-to-width of 6, 8 and 10 and crack length to width ratios between 0.1 and 0.6. Strain hardening levels of 5, 10 and 20 were selected to observe the effect of high (n=5) and low (n=20) material was also investigated. Finally, the level of crack tip stress triaxiality in this specimen configuration was determined and compared with standard specimens.

Expressions for compliance stress intensity and η_{pl} are presented in a format that is consistent with ASTM standards for other specimen geometries. Results indicate that η_{pl} increases with strain hardening for a/W<0.40 and with H/W at crack lengths >0.30 and that strain hardening has a larger overall effect on η_{pl} than H/W. Furthermore, clamped end short crack SE(T)s can provide more crack tip triaxiality than short crack SE(B)s and possibly approximate the constraint and loading condition within a structure of interest..

14. SUBJECT TERMS
Fracture Testing, SE(T), Constraint, Plastic Eta Factor, Fixed End Loading, Single Edge Tension, Compliance, Stress Intensity Factor, H/W Effects

15. NUMBER OF PAGES
22

16. PRICE CODE

17. SECURITY CLASSIFICATION OF REPORT	18. SECURITY CLASSIFICATION OF THIS PAGE	19. SECURITY CLASSIFICATION OF ABSTRACT	20. LIMITATION OF ABSTRACT
Unclassified	Unclassified	Unclassified	Unclassified

Table of Contents

List of Figures

List of Tables

Abstract

An analysis of single edge cracked tension specimens with clamped end conditions was conducted. Single edge tension finite element models at nine crack lengths were constructed and benchmarked against previously accepted analyses with pinloaded boundary conditions. The model boundary conditions were then determined by a direct comparison with experimental strain and displacement data from clamped end specimens. Both the elastic (compliance and elastic stress intensity) and the plastic response (J-plastic, η_{pl}) of the clamped end model were determined at ratios of height-to-width of 6, 8 and 10 and crack length to width ratios between 0.1 and 0.6. Strain hardening levels of 5, 10 and 20 were selected to observe the effect of high (n=5) and low (n=20) material was also investigated. Finally, the level of crack tip stress triaxiality in this specimen configuration was determined and compared with standard specimens.

Expressions for compliance stress intensity and η_{pl} are presented in a format that is consistent with ASTM standards for other specimen geometries. Results indicate that η_{pl} increases with strain hardening for a/W<0.40 and with H/W at crack lengths >0.30 and that strain hardening has a larger overall effect on η_{pl} than H/W. Furthermore, clamped end short crack SE(T)s can provide more crack tip triaxiality than short crack SE(B)s and possibly approximate the constraint and loading condition within a structure of interest.

Administrative Information

The work performed herein was sponsored by the Office of Naval Research 6.2 Ship and Submarine Materials Technology Block program managed by Dr. William Messick, CDNSWC (0115). The effort was conducted under program element 602234N, work unit 1-6140-254-10 and was supervised by Mr. T. W. Montemarano, Head, Fatigue and Fracture Branch (Code 614).

Introduction

Single edge crack tension (SE(T)) specimens are frequently used in fracture and fatigue testing, and there is an abundance of published work [1,2,3] describing various test procedures. Short crack SE(T) specimens provide a reasonable approximation to a structural test, particularly in welded structures where flaws may concentrate near the surface. While a structural test may require extensive analysis, SE(T) geometry is simple and easily modeled using finite element analysis. Historically, SE(T)s specimens were pin loaded. However, this geometry requires a specimen wide enough to avoid failure at either the specimen bearing surface or the pin itself. Specimens in which the crack propagates through the plate thickness (T-S or L-S) are especially problematic since the width of the specimen is limited by the plate thickness. To alleviate this problem SE(T) specimen can be tested using wedge grips which clamp the specimen ends.

An illustration of a wedge gripped SE(T) is shown in Figure 1. The schematic shows the top and bottom 20% of the total specimen length clamped in wedge grips and displaced uniformly throughout the gripped area. Here, unlike pin loading where the ends are free to rotate and the crack can open unhindered, the presence of the crack shifts the line of action away from the specimen centerline. This shift produces a bending moment that attempts to close the crack causing the stress distribution imposed on the specimen to be a function of x, a/W, and H/W as defined in Figure 1. While many authors have studied the effect of this end condition [1-4]; no detailed study has been done producing both elastic and plastic results that can be used in a standard test format. Stress intensity (K), compliance and plastic J-Integral solutions for pin loaded specimens have been published in a standard format [5]. However, the non-uniform stress

distribution of the clamped-end specimen precludes the use of these results. Further, constraint effects for this loading condition are not characterized, making it difficult to correlate J-Integral results with values from standard test geometries. Therefore, new compliance, K and plastic J-Integral solutions for clamped end SE(T) specimens were developed using finite element analysis.

This paper describes the analysis performed to develop new K, compliance and J-Integral solutions. Thirty finite element analyses were conducted at 6 crack lengths, 3 hardening coefficient (n) values and 3 height-to-width ratios as summarized in Table 1. The boundary conditions of these models were validated by direct comparison with strain gage measurements. Finally, published small-scale yielding modified boundary layer analyses were used to calculate constraint loss in the form of J-Q trajectory plots [6-7].

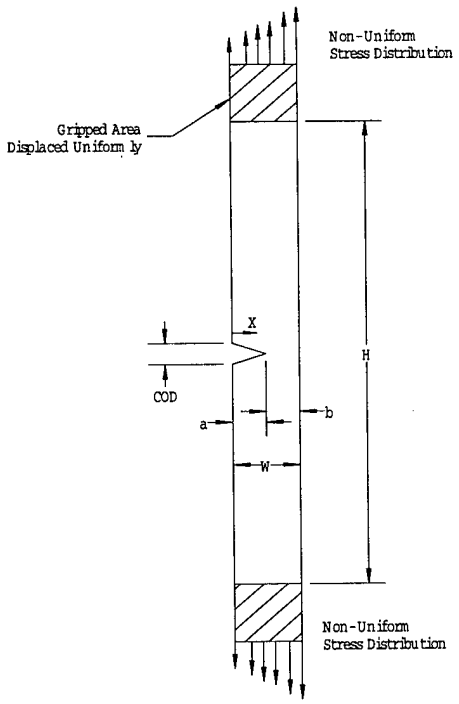

Figure 1
Fixed End SE(T) Geometry

H/W	n	a/W
6	10	0.10 – 0.60
8	5, 10, 20	0.10 – 0.60
10	10	0.10 – 0.60

Table 1
Summary of Various Finite Element Models

Finite Element Model Verification

The commercial finite element package ABAQUS was used to calculate compliance, K and plastic J-Integrals solutions for lengths ranging from a/W of 0.10 to 0.60. One model at a/W of 0.10 was used to determine J-Q trajectories for comparison with other well known solutions of pin-loaded SE(T) and short crack single edge bend (SE(B)) specimens [8]. A typical model has 1000 to 1500 eight noded plain strain reduced integration elements with 15 to 20 elements along the two-inch width of the specimen. Mesh studies indicated that a minimum of 10 elements is required to capture variation in strain along the width of the specimen. The 20-inch specimens were modeled using the half symmetry as shown in Figure 2 making the total model length 10-inches. Loading was accomplished by displacing all nodes along the top edge for H/W of 10 and top 2 and 4 inches for H/Ws of 8 and 6 respectively. Elements in the gripped area are modeled as fully elastic to save computational time and distribute the loading effectively. A symmetry boundary condition was applied to the elements along the remaining ligament along the same plane that contained the crack. A keyhole with a 0.0005-inch radius, shown in Figure 3, is used to model the crack tip for both elastic and elastic-plastic solutions. To resolve stresses near the crack tip, the keyhole was collapsed into a single point and crack tip element sizes reduced by ½ to construct the focused, refined mesh used for the J-Q trajectory calculation. Typically, forty to sixty radial rings of elements

surround the crack tip, gradually increasing in size from 0.00025-inch at the keyhole to .05-inch at the last ring. Each ring contained 24 elements dispersed equally around the keyhole. All nodes along the keyhole radius, with the exception of the one node that was on the symmetry plane, were unconstrained to simulate blunting behavior.

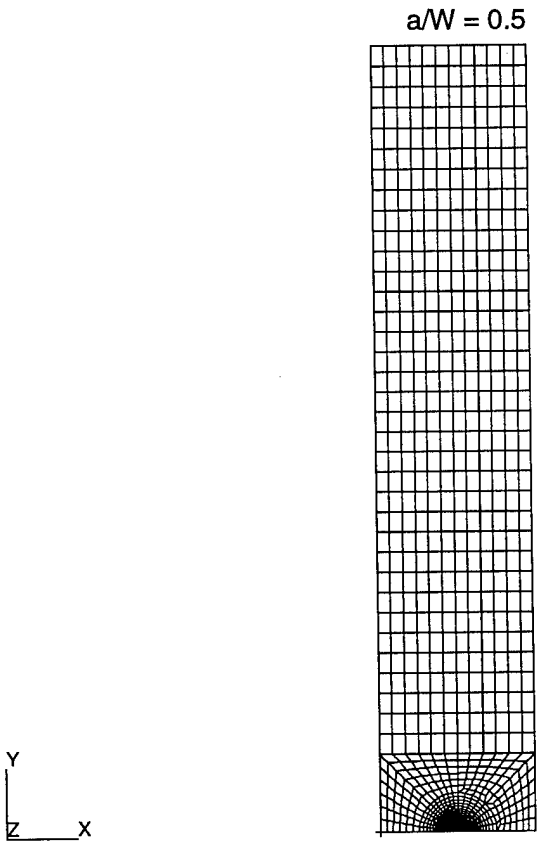

Figure 2
Typical SE(T) Finite Element Model Using ½ Symmetry

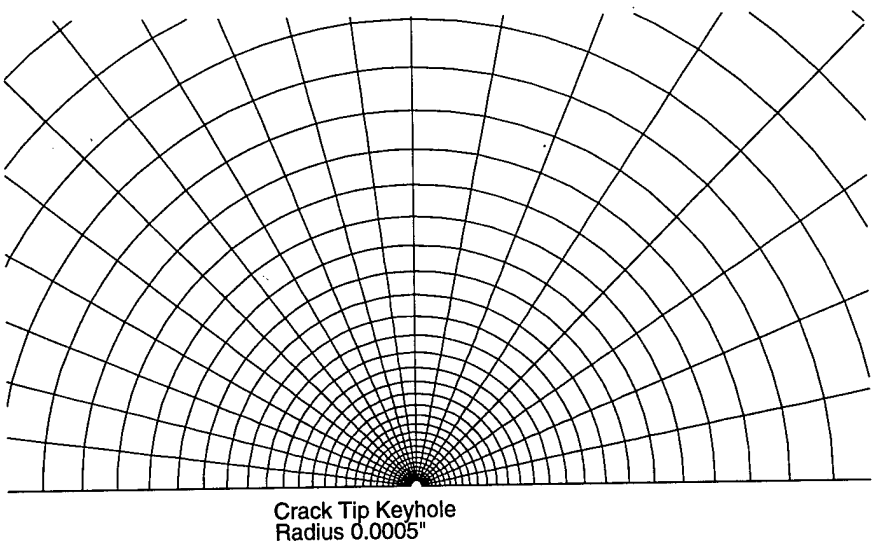

Figure 3
Finite Element Model Crack Tip

Mesh Verification

Prior to modeling clamped end loading, the accuracy of the finite element model and data reduction techniques were verified by reproducing accepted solutions for pin loaded SE(T)s. Nine finite element models were displaced to a loadline displacement (Δ_{LL}) of 0.02 inches at a point 9 inches above the crack plane along the specimen centerline. All elements for this initial analysis were defined as linear elastic as shown in Table 2 on page 8. Load (P) and elastic J-Integral (J_{el}) values were computed at the end of each loading. Compliance estimates, normalized by the plane strain elastic modulus (E') and the specimen thickness (B), are shown in Figure 4. The normalized compliances (BE'C) predicted from this analysis display little deviation from the predicted handbook

values [9] or prior finite element studies [5]. This result confirms that the model boundary conditions correspond to pin-loaded end conditions with uniform stress.

To ensure that the mesh was suitable for fracture analysis, J_{el} values were compared with values calculated by Tada [9] and Joyce [5]. J_{el} is defined as:

$$J_{el} = \frac{K^2}{E'} \qquad \text{Where } K = \sigma\sqrt{\pi a}F(a/W) \tag{1}$$

In Equation 1, F(a/W) is a geometry dependent function of normalized crack length, σ is the remote stress and a is the crack length. While J_{el} can be determined with a relatively coarse mesh, gross variation in values from the reference values would indicate a problem with crack definition or boundary conditions. Figure 5 reveals excellent correlation with both Tada and Joyce at each modeled crack length. Variations from handbook values are less than 1% for all a/W.

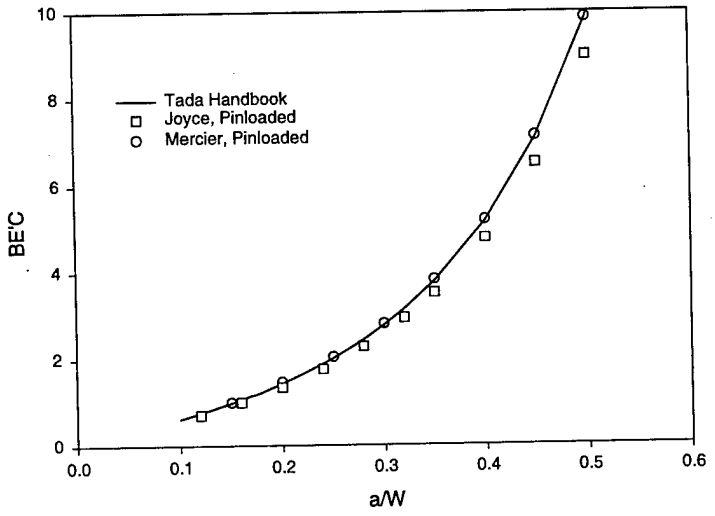

Figure 4
Comparison of Pinloaded SE(T) Compliance

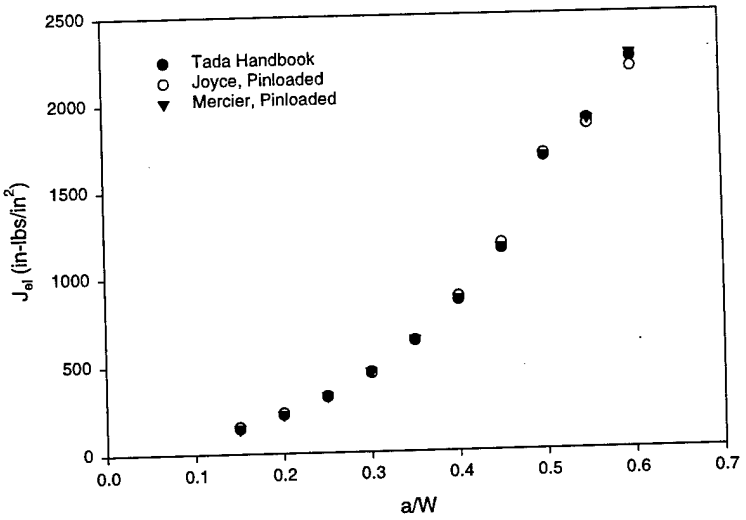

Figure 5
Comparison of Pinloaded SE(T) J_{el}

Mesh refinement and crack tip geometry were verified by comparison of η_{pl} with published results from references 5 and 10. Loading and boundary conditions for all a/W were maintained the same as in the previous elastic analysis. However, the plastic response of the models was defined by the Ramberg-Osgood coefficients shown in Table 2. Elements within the top 20% of the model were defined as elastic for reasons previously stated. Each loading was separated into 20 steps. At each step, load, load-line displacement and J-Integral values were determined and the plastic area (A_{pl}) and J_{pl} were calculated. A_{pl} is defined by:

$$A_{pli} = \frac{(P_{i-1} + P_i)}{2}(\Delta_{i-1}^{LLpl} - \Delta_i^{LLpl}) \quad \text{and} \quad (2)$$

$$J_{pl} = J_{total} - J_{el} \quad (3)$$

Where J_{el} was found using Equation 1

The plastic eta factor, η_{pl}, is defined as:

$$\eta_{pl} = \frac{J_{pl} B_N b}{A_{pl}} \quad (4)$$

If J_{pl} is normalized by the flow stress (σ_0) and remaining ligament (b) and A_{pl} normalized by the net thickness (B_N), b and σ_0, then η_{pl} can be determined by the slope of the normalized J_{pl} vs. A_{pl} curve.

$$\eta_{pl}\frac{A_{pl}}{B_N b^2 \sigma_o} = \frac{J_{pl}}{b\sigma_o} \tag{5}$$

The normalized values of J_{pl} and A_{pl} are plotted for a/W=0.5 in Figure 6. Each of the 9 crack lengths was analyzed with this method and the results are plotted in Figure 7 along with results for Joyce [5] and EPRI [10]. Joyce used a piecewise stress-strain curve to define HY-100 material properties while EPRI results are based on the same Ramberg-Osgood relations used in this study. Joyce's HY-100 model has a hardening coefficient of approximately n=14. A comparison of the three analyses confirms that the crack tip geometry, mesh refinement and data reduction techniques are suitable.

Analysis	Modulus (psi)	Poisson's ratio	Yield Stress (psi)	Strain Hardening Coefficient (n)	Yield Point Offset (α)
Elastic, Plastic Solutions	29E6	0.3	100000	5, 10, 20	0.5
Boundary Condition Validation	29E6	0.3	Piecewise Linear Material Stress-Strain Data Shown in Figure 8, n≈15		
J-Q Trajectories	50E6	0.3	100000	10	0.5

Table 2
Material Properties Used in Finite Element Models

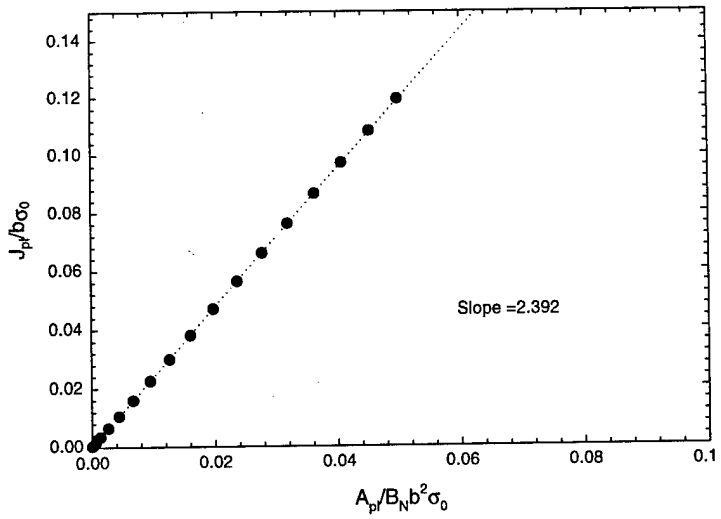

Figure 6
η_{pl} Analysis of Pinloaded SE(T) at a/W=0.5

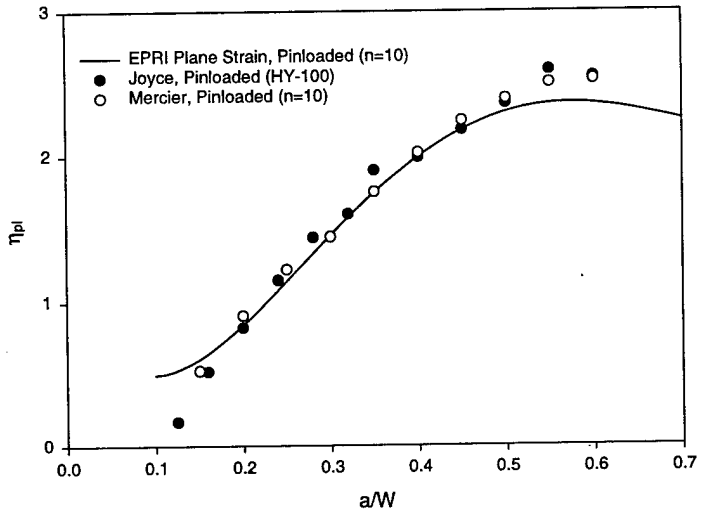

Figure 7
Comparison of η_{pl} for Pinloaded SE(T)

Clamped End Boundary Condition Validation

Clamped end SE(T) specimens are subjected to non-uniform stresses created by the presence of the edge crack. These stresses create bending moments that act to close the crack. The complexities of the clamped end conditions makes it necessary to first

compare measured specimen response with model response and then revise the model end conditions until sufficient agreement is achieved. Mesh design, crack tip geometry and symmetry conditions remained unchanged from the previous pin-loaded analysis. Material property data was changed as indicated in Table 2 and loading conditions were changed to replicate measured strains.

Two HSLA-100 test specimens with an a/W of 0.15 were strain gaged as shown in Figure 9. Placement of the gages was selected to capture the variation in strain along the width of the specimen. Prior testing showed that strains were symmetric about the crack plane, and that no out-of-plane bending occurred. The specimens were fatigue precracked in three point bending as per reference [11] then placed in a 300 kip capacity screw driven machine for testing. Crack extension was monitored via unloading compliance and the test was terminated when crack extension exceeded 0.200 inches, or the clip gage used to measure compliance reached full scale. Unloadings were subsequently removed from the data to provide load-displacement and load-strain comparison.

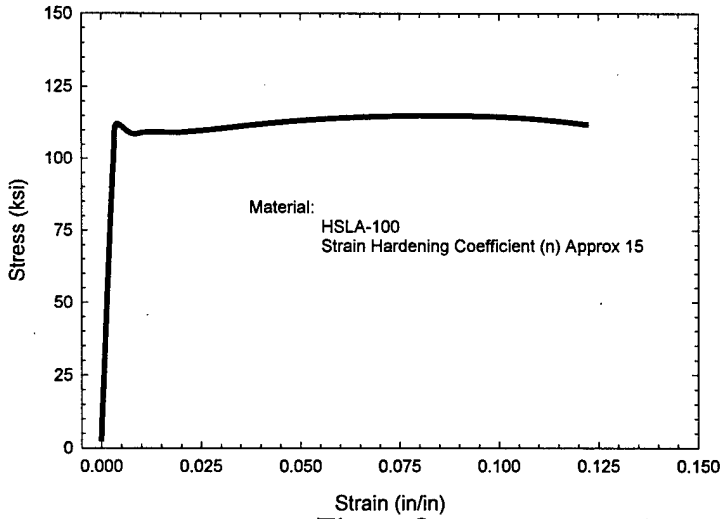

Figure 8
Stress Strain Properties Used in Boundary Condition Validation

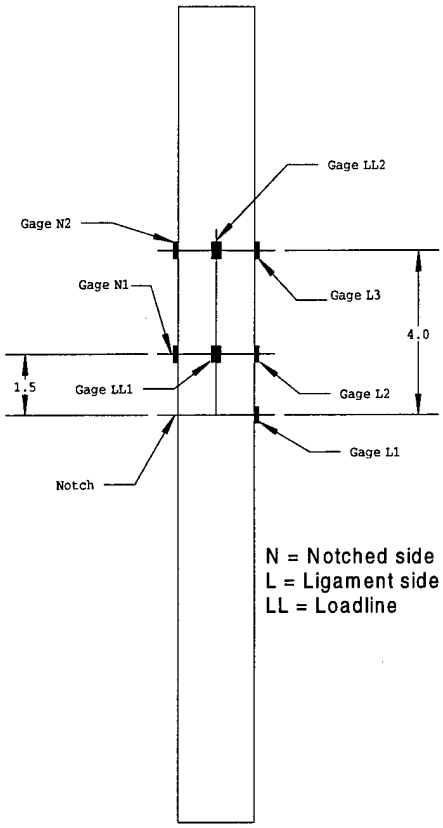

Figure 9
Specimen Schematic Showing Strain Gage Location

The finite element model with a/W = 0.15 was used to verify the boundary conditions by comparing predicted strain, load and COD with measured values. Figure 10 clearly shows good agreement between the measured and predicted load versus COD curves. The plane-strain finite element results slightly over-estimate material hardening. However, this is not unexpected since plane strain conditions do not exist throughout the specimen thickness. A full three-dimensional analysis would be required to accurately predict load-COD and strain levels. Results from both predicted and experimental strains are shown in Figure 11. The bending created by the clamped ends is evident. Ligament side strains are elevated well above notch or load line strains. As with the load-COD

results, the predicted strains are elevated due to the choice of plane strain elements. Clearly, the computational results follow the experimental trends, thereby lending confidence in the finite element model.

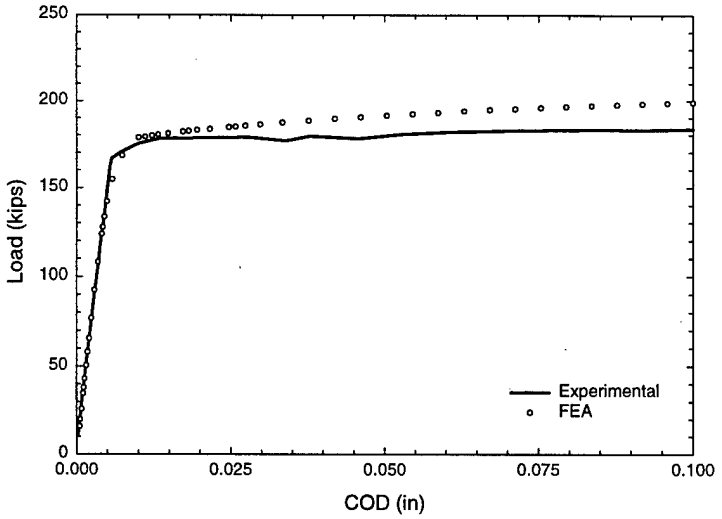

Figure 10
Comparison of Measured and Predicted Load-COD Values

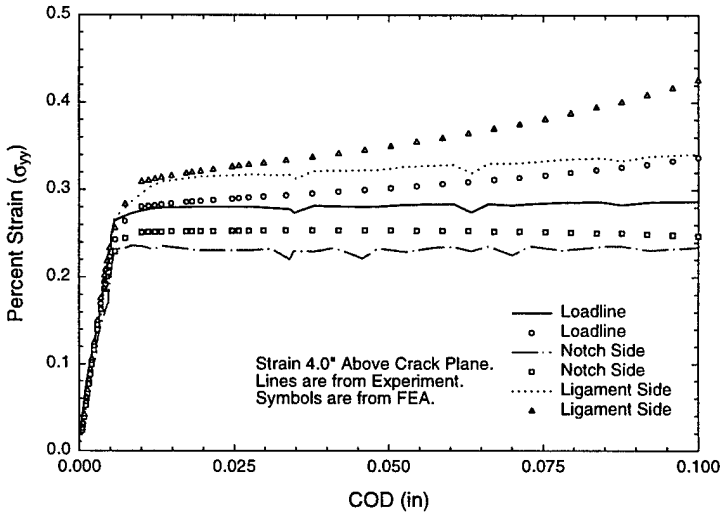

Figure 11
Comparison of Measured and Predicted Strains

Clamped End Analysis Results and Discussion

Elastic Analysis

John and Rigling [4] provide an in-depth analysis of the elastic response of a clamped-end SE(T) for multiple a/W and H/W. Their results are easily converted to standard ASTM format for automated testing. They showed that K solutions for clamped end loading are bounded by K solutions for double edge cracked geometry for small height-to-width ratios and pin loaded SE(T) solutions for large H/W. Furthermore, there is a pronounced H/W effect at deeper crack length. At a/W greater than 0.40, normalized stress intensity results for H/W of 10 can be twice the normalized K at H/W of 2. The same H/W sensitivity is seen in compliance results. Comparisons of John and Rigling's elastic results with the current analysis at one H/W are shown for both compliance and stress intensity factor in Figure 12 and Figure 13 respectively. Equations in standard format are also included in each figure. Results at other values of H/W show similar agreement; therefore, J-elastic is calculated using reference 4 in all further analysis.

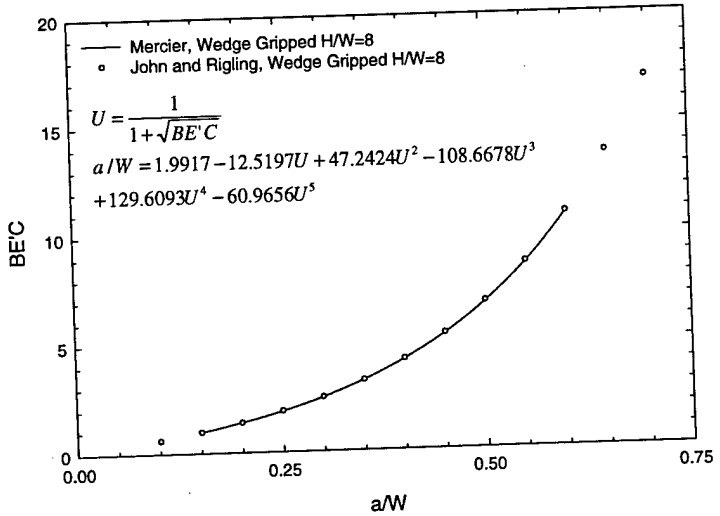

Figure 12
Comparison of Compliance Results for Clamped End SE)T) at H/W=8

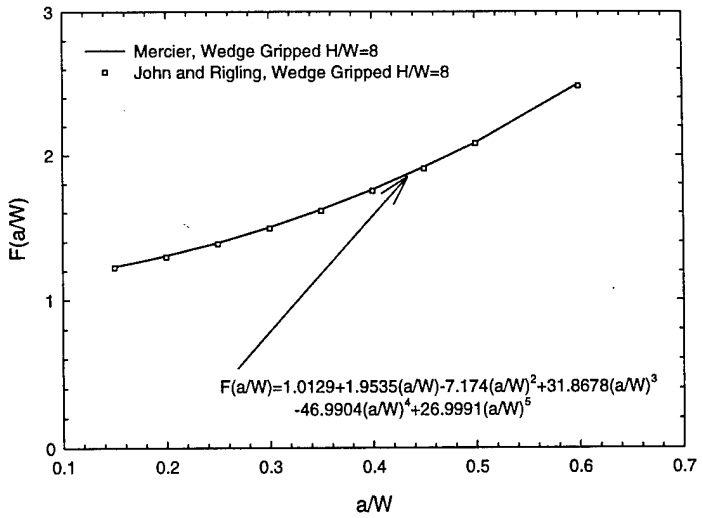

Figure 13
Comparison of Stress Intensity Factor Relationships for Clamped End SE(T) at H/W=8

Plastic Analysis

Thirty finite element analyses were conducted to investigate both H/W and strain hardening effects on η_{PL} (see Table 3). The values of H/W selected were common values that typically might be used in testing. The analysis considered a range of flow properties ranging from low strain hardening (n=20) to high strain hardening (n=5). Figure 14 shows that for short cracks (a/W<0.4) η_{pl} exhibits a strong dependence on n whereas for longer crack lengths (a/W > 0.5)it is insensitive to strain hardening. This effect has been shown for many crack geometries, including pin-loaded SE(T)s [12].

Strain hardening dominates η_{PL} at shorter crack lengths. However, as shown in Figure 15, increasing H/W increases η_{PL} at longer crack lengths (a/W>0.3). In fact, it is expected that for H/W>>10, η_{pl} for a wedge gripped SE(T)s would resemble η_{pl} for pin loading since the stress fields would tend to be uniform over the central ligament. While H/W does influence η_{PL}, its effect is not as severe as strain hardening. Moreover, within

the range of a/W and H/W studied, the greatest variation in η_{PL} due to H/W was 13% (H/W=6 and H/W=10 at a/W=0.6) while n varied η_{PL} by more than 60% at a/W=0.1.

a/W	H/W=6, n=10	H/W=8, n=10	H/W=10, n=10	H/W=8, n=5	H/W=8, n=20
0.1	0.345	0.344	0.344	0.212	0.600
0.2	0.809	0.810	0.810	0.535	1.010
0.3	1.005	1.027	1.055	0.852	1.060
0.4	1.010	1.052	1.090	1.015	1.055
0.5	0.934	0.970	1.030	0.965	0.984
0.6	0.864	0.910	0.981	0.894	0.930

Table 3
Predicted η_{pl} Factors for Clamped End SE(T)s at Various H/W and a/W

Piecewise linear functions are standard way to calculate η_{pl} during a test [11]. Below are functions that can be used for the data in Table 3.

H/W=6, n=10:

$0.1 \le a/W \le 0.3$ $\quad \eta = 3.3a/W + 0.6$

$0.3 < a/W \le 0.4$ $\quad \eta = 0.05a/W + 0.99$

$0.4 < a/W \le 0.6$ $\quad \eta = -0.73a/W + 1.3$

H/W=8, n=10:

$0.1 \le a/W \le 0.3$ $\quad \eta = 3.3a/W + 0.6$

$0.3 < a/W \le 0.4$ $\quad \eta = 0.05a/W + 0.99$

$0.4 < a/W \le 0.6$ $\quad \eta = -0.73a/W + 1.3$

H/W=10, n=10:

$0.1 \le a/W \le 0.3$ $\quad \eta = 3.56a/W + 0.97$

$0.3 < a/W \le 0.4$ $\quad \eta = 0.35a/W + 0.95$

$0.4 < a/W \le 0.6$ $\quad \eta = -0.55a/W + 1.31$

H/W=8, n=5:

$0.1 \le a/W \le 0.4$ $\quad \eta = 2.73a/W - 0.03$

$0.4 < a/W \le 0.6$ $\quad \eta = -0.61a/W + 1.26$

H/W=8, n=20:

$0.1 \le a/W \le 0.2$ $\quad \eta = 4.1a/W + 0.19$

$0.2 < a/W \le 0.4$ $\quad \eta = 0.26a/W + 0.97$

$0.4 < a/W \le 0.6$ $\quad \eta = -0.63a/W + 1.3$

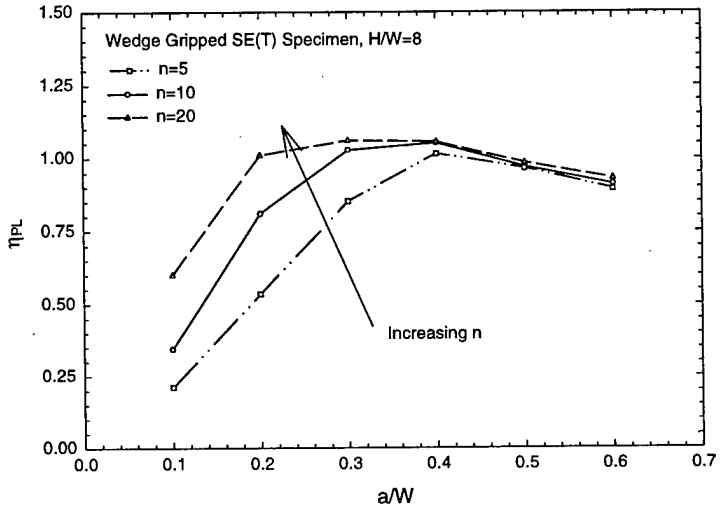

Figure 14

Predicted η_{pl} Factors for Clamped End SE(T) Specimens at Constant H/W

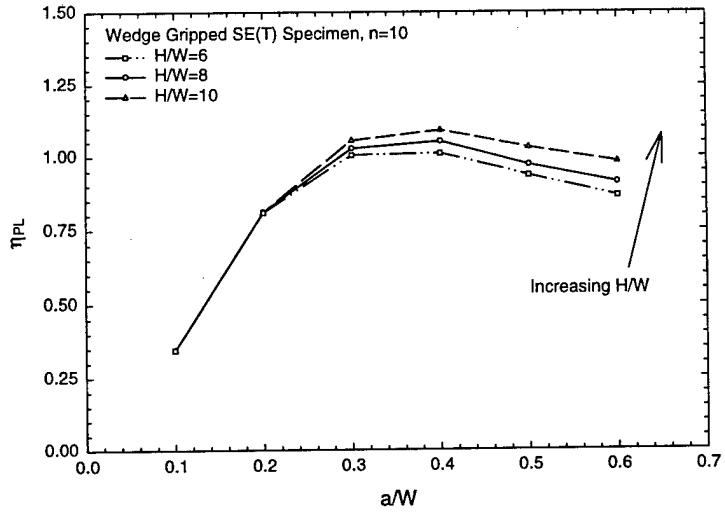

Figure 15
Predicted η_{pl} Factors for Clamped End SE(T) Specimens at Constant Strain Hardening

Summary of η_{pl} Results

This report presents compliance, K and plastic J solutions for the clamped-end SE(T) specimen over a range of $0.1 < a/W < 0.6$, $6 < H/W < 10$ and $5 < n < 20$. Results are presented in a format that is consistent with ASTM standards for other specimen geometries. The following effects have been shown to occur in clamped end SE(T) specimens:

- η_{pl} increases with strain hardening for $a/W<0.40$.
- η_{pl} increases with H/W at crack lengths >0.30.
- Strain hardening has a larger overall effect on η_{pl} than H/W.

Constraint

The finite element model used to investigate constraint consisted of 3000 8 noded, reduced integration quadratic elements. Twenty-four quad elements were collapsed into

triangles forming a focused mesh at the crack tip. Fifty concentric rings of elements surrounded the tip. The mechanical properties used in this analysis are shown in Table 2. These properties were selected for direct comparisons with J-Q results from Gullerud and Dodds [8]. Crack tip constraint can be characterized by both the near tip deformation and the level of triaxiality ahead of the crack tip. J defines the deformation and the non-dimensional Q stress quantifies the triaxiality. Q is defined as:

$$Q = \frac{\sigma_{YY(FEA)} - \sigma_{YY}}{\sigma_0} \tag{5}$$

Where $\sigma_{YY(FEA)}$ is predicted finite element strains ahead of the crack tip and σ_{YY} is results from a modified boundary layer analysis preformed by Gullerud and Dodds [7]. Results from [7] show that, as deformation levels increase, the short crack pin-loaded SE(T) specimen loses constraint quicker than the single edge bend (SE(B)) specimen of the same crack length. These two geometries are compared to the wedge gripped SE(T) in Figure 16. It is clear from this plot that for short cracks (a/W = 0.10), clamped end loading adds constraint to the specimen since the wedge gripped SE(T) maintains higher levels of triaxiality than the SE(B) geometry. As before, if the H/W ratio were increased above 10, it is believed that the clamped grip loading would resemble pin-loading. Furthermore, other authors have shown that as strain hardening increases, constraint decreases rapidly [13], and as a/W increases constraint increases [8,13].

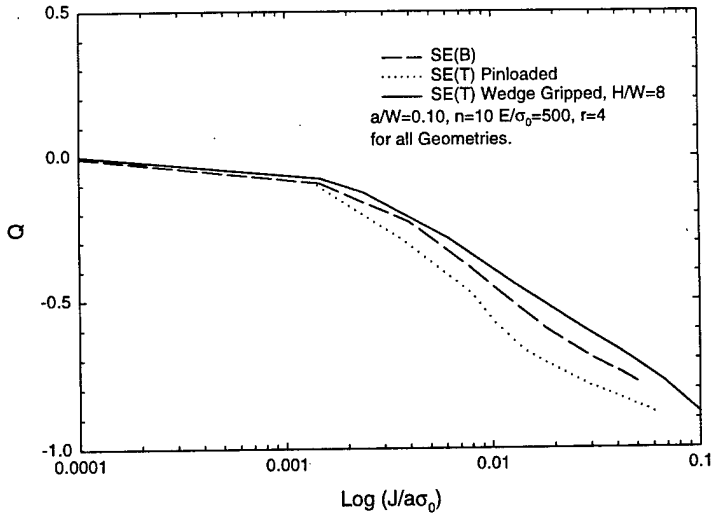

Figure 16
Comparison of J-Q Trajectories for Short Crack, Clamped End SE(T), Pin-Loaded SE(T) and SE(B) Specimens

Conclusion

Conclusions from this study are:

- Clamped end short crack SE(T)s can provide more crack tip triaxiality than short crack SE(B)s.
- Selection of appropriate a/W and H/W will provide constraint levels within the specimen that can closely approximate constraint within a structure of interest.
- In clamped end SE(T) specimens η_{pl} increases with strain hardening for a/W<0.40.
- In clamped end SE(T) specimens η_{pl} increases with H/W at crack lengths >0.30.
- In clamped end SE(T) specimens strain hardening has a larger overall effect on η_{pl} than H/W.

References

1 Ahmad, J., Papaspyropoulos, V. and Hopper, A. T., "Elastic-Plastic Analysis of Edge-Notched Panels Subjected to Fixed Grip Loading." *Engineering Fracture Mechanics*, Vol. 38, pp. 283-294, 1991.

2 Marchand, N., Parks, D. M. and Pelloux, R. M., "K_I-Solutions for Single Edge Notch Specimens Under Fixed End Displacements." *International Journal of Fracture*, Vol. 31, pp. 53-65, 1986.

3 Dao, T. X. and Mettu, S. R., "*Analysis of an Edge-cracked Specimen Subjected to Rotationally Constrained End Displacements*." NASA JSC 32171, 1991.

4 John, R. and Rigling, B., " Effect of Height to Width Ratio on K and CMOD Solutions for a Single Edge Cracked Geometry with Clamped Ends." *Engineering Fracture Mechanics*, Vol. 60, No. 2, pp. 147-156, 1998.

5 Joyce, J. A., Hackett, E. M., and Roe, C., " Effect of Crack Depth and Mode of Loading on the J-R Behavior of a High-Strength Steel." *Constraint Effects in Fracture ASTM STP 1171,* E. M. Hackett, K. H. Schwalbe, and R. H. Dodds, Eds., ASTM, Philadelphia, 1993, pp. 239-263.

6 Dodds, R. H., Shih, C. F. and Anderson, T. L., "Continuum and Micro-Mechanics Treatment of Constraint in Fracture," *International Journal of Fracture*, Vol 64, pp. 101-133, 1993.

7 Nevalainen, M. and Dodds, R. H., "Numerical Investigation of 3-D Constraint Effects on Brittle Fracture in SE(B) and C(T) Specimen," *International Journal of Fracture*, Vol 74, pp. 131-161, 1995.

8 Gullerud, A. S., and Dodds, R. H. "J-Q and Toughness Scaling Model Solutions for M(T), DE(T), SE(B), SE(T) and C(T) Specimens," NUREG/CR-6831, U.S. Nuclear Regulatory Commission, Washington D.C., 1995.

9 Tada, H., Paris, P. C., and Irwin, G. R., *The Stress Analysis Handbook*, Paris Productions, Inc., St. Louis, 1985.

10 Kumar, V., German, M. D. and Shih, C. F., *An Engineering Approach to Elastic-Plastic Fracture*, EPRI NP-1931, Electric Power Research Institute, Palo Alto, 1981.

11 ASTM E1820-96, "Standard Test Method for Measurement of Fracture Toughness," ASTM, Philadelphia, 1996.

12 Wu, S. X., Mai, Y. W. and Cotterell, B. "Plastic η Factors for Specimens With Deep and Shallow Cracks," *International Journal of Fracture*, Vol 45, pp. 1-18, 1990.

13 Wu, S., Mai, Y. and Cotterell, B. "Q Solutions for Compact Tension and Single-Edge Cracked Tension Specimens," *International Journal of Fracture*, Vol. 68, pp. R97-R103, 1995.

DISTRIBUTION LIST

Outside Distribution

Copies	Agency
6	NAVSEA
1	SEAO3M
1	SEAO8s
1	SEA 03M2 (Null)
1	SEA 03P (McCarthy)
1	SEA 03P2 (Nichols)
1	SEA 03P4 (Manuel)
2	DTIC
3	ONR
1	1131 (Yoder)
1	1131 (Sedricks)
1	332 (Vasudevan)
1	NRL
1	Code 6310

Center Distribution

Copies	Code
1	0115 (Messick)
1	60 (Wacker)
1	601 (Morton)
1	602 (Rockwell)
1	603 (Cavallaro)
1	604 (DeSavage)
1	605 (Fisch)
1	61 (Holsberg)
1	61s
1	62 (Eichenger)
1	63 (Alig)
1	64 (Fischer)
1	65 (Beach)
1	66 (Riley)
1	67 (Hansen)
1	68 (Sudduth)
1	611 (Palko)
1	612 (Aprigliano)
1	613 (Ferrara)
1	614 (Montemarano)
1	614 (Czyryca)
1	614 (Tregoning)
1	614 (Graham)
1	614 (McKirgan)
15	614 (Mercier)
1	614s
1	615 (DeNale)
1	3421